
UNIVERSITY
OF WOLLONGONG
AUSTRALIA

University of Wollongong
Research Online

Faculty of Engineering and Information Sciences - Papers: Part A

Faculty of Engineering and Information Sciences

2014

Dynamic conductivity of the bulk states of n-type HgTe/CdTe quantum well topological insulator

Qinjun Chen
University of Wollongong, qc691@uowmail.edu.au

Matthew Sanderson
University of Wollongong, ms919@uowmail.edu.au

J C. Cao
Shanghai Institute of Microsystem and Information Technology

Chao Zhang
University of Wollongong, czhang@uow.edu.au

Publication Details

Chen, Q., Sanderson, M., Cao, J. C. & Zhang, C. (2014). Dynamic conductivity of the bulk states of n-type HgTe/CdTe quantum well topological insulator. Applied Physics Letters, 105 202110-1-202110-5.

Research Online is the open access institutional repository for the University of Wollongong. For further information contact the UOW Library: research-pubs@uow.edu.au

Dynamic conductivity of the bulk states of n-type HgTe/CdTe quantum well topological insulator

Abstract
We theoretically studied the frequency-dependent current response of the bulk state of topological insulator HgTe/CdTe quantum well. The optical conductivity is mainly due to the inter-band process at high frequencies. At low frequencies, intra-band process dominates with a dramatic drop to near zero before the inter-band contribution takes over. The conductivity decreases with temperature at low temperature and increases with temperature at high temperature. The transport scattering rate has an opposite frequency dependence in the low and high temperature regime. The different frequency dependence is due to the interplay of the carrier-impurity scattering and carrier population near the Fermi surface.

Disciplines
Engineering | Science and Technology Studies

Publication Details
Chen, Q., Sanderson, M., Cao, J. C. & Zhang, C. (2014). Dynamic conductivity of the bulk states of n-type HgTe/CdTe quantum well topological insulator. Applied Physics Letters, 105 202110-1-202110-5.

This journal article is available at Research Online: http://ro.uow.edu.au/eispapers/3377

Dynamic conductivity of the bulk states of n-type HgTe/CdTe quantum well topological insulator

Qinjun Chen, Matthew Sanderson, J. C. Cao, and Chao Zhang

Citation: Applied Physics Letters **105**, 202110 (2014); doi: 10.1063/1.4902411
View online: http://dx.doi.org/10.1063/1.4902411
View Table of Contents: http://scitation.aip.org/content/aip/journal/apl/105/20?ver=pdfcov
Published by the AIP Publishing

Articles you may be interested in

Thermoelectric properties of two-dimensional topological insulators doped with nonmagnetic impurities
J. Appl. Phys. **116**, 013706 (2014); 10.1063/1.4886176

Energy loss rate of a charged particle in HgTe/(HgTe, CdTe) quantum wells
Appl. Phys. Lett. **103**, 192107 (2013); 10.1063/1.4829467

Design principles for HgTe based topological insulator devices
J. Appl. Phys. **114**, 043702 (2013); 10.1063/1.4813877

Photomixing in topological insulator HgTe/CdTe quantum wells in terahertz regime
Appl. Phys. Lett. **101**, 211109 (2012); 10.1063/1.4768781

Enhanced numerical analysis of current-voltage characteristics of long wavelength infrared n-on-p HgCdTe photodiodes
J. Appl. Phys. **108**, 074519 (2010); 10.1063/1.3483926

This article is copyrighted as indicated in the article. Reuse of AIP content is subject to the terms at: http://scitation.aip.org/termsconditions. Downloaded to IP: 130.130.37.85 On: Wed, 26 Nov 2014 03:48:51

Dynamic conductivity of the bulk states of n-type HgTe/CdTe quantum well topological insulator

Qinjun Chen,[1] Matthew Sanderson,[1] J. C. Cao,[2] and Chao Zhang[1,3,a)]
[1]*School of Physics, University of Wollongong, New South Wales 2522, Australia*
[2]*Key Laboratory of Terahertz Solid State Technology, Shanghai Institute of Microsystem and Information Technology, Chinese Academy of Sciences, Shanghai, China*
[3]*Cooperative Innovation Centre of Terahertz Science, Chengdu, Sichuan 610054, China*

(Received 27 August 2014; accepted 12 November 2014; published online 20 November 2014)

We theoretically studied the frequency-dependent current response of the bulk state of topological insulator HgTe/CdTe quantum well. The optical conductivity is mainly due to the inter-band process at high frequencies. At low frequencies, intra-band process dominates with a dramatic drop to near zero before the inter-band contribution takes over. The conductivity decreases with temperature at low temperature and increases with temperature at high temperature. The transport scattering rate has an opposite frequency dependence in the low and high temperature regime. The different frequency dependence is due to the interplay of the carrier-impurity scattering and carrier population near the Fermi surface. © *2014 AIP Publishing LLC*.
[http://dx.doi.org/10.1063/1.4902411]

Topological insulators (TIs) are a sort of bulk insulators with strong intrinsic spin orbit coupling, which leads to the formation of topological edge (in two dimensional, 2D) or surface (in three dimensional, 3D) states that are ambipolar metallic Dirac cone structure.[1–5] These Dirac cones are well protected by the time reversal symmetry and exhibit peculiar properties such as intrinsic quantum spin Hall effect,[2,6] dissipationless transport property,[7] and spin texture determined by the direction of momentum due to the spin-momentum lockage.[8] Since graphene has been proven to be a failure as TI material owing to the weak spin orbit coupling,[9,10] Bernevig *et al.*[2] proposed a prediction that HgTe/CdTe QW could be an ideal 2D TI, which was soon proved by Konig *et al.*[6] in experiment in 2007. In HgTe/CdTe QW, two CdTe barrier layers sandwich on one HgTe layer, constructing a 2D electron gas (2DEG) confined in the 2D HgTe "well." In this system, the energy gap of the electron band structure is controllable by modifying the thickness of HgTe "well."[6,11] For example, when the thickness of the "well" increases up to a critical value, 6.3 nm, there appears an inverted band structure, where the *s*-like Γ_6 band is pulled down below the *p*-like Γ_8 band because of the enhanced strong spin obit coupling.[2,12] In the inverted band regime, the measured plateau of residual conductance was very close to the predicted value $2e^2/h$, where e is the electron charge, and h is the plank's constant.[6]

There has been a myriad of research, both experimentally and theoretically, focusing on electron transports of the surface and bulk state of TIs.[13–19] However, when proceeding transport measurements of the topological edge or surface, the bulk response would significantly interrupt the surface signal. The response from the bulk would certainly be annoying if one cannot distinguish the different between the edge or surface and bulk. It has been suggested[20] that in order to access the surface properties, the chemical potential should be confined within the bulk gap and right on the Dirac point. Kim *et al.*[5] demonstrated a gate electrode to control the bulk carrier density of Bi_2Se_3, where surface transport was strongly electrostatically coupled when the bulk carriers were removed completely. Another efficient way to tune the Fermi level into the bulk gap is by doping. Successful examples have been reported on Ca, Sb, and Mg doped Bi_2Se_3 and Sn doped Bi_2Te_3.[21–24]

However, our interest will be focused on 2D HgTe/CdTe QW TIs, on which the edge state is one dimensional. It has been reported that the carrier density of HgTe/CdTe QW can be reduced to the magnitude of $\sim 10^{11}\,\mathrm{cm}^{-2}$ in a highly pure sample.[6] Even in such low carrier density system, we noticed that in the case of $d = 7.0$ nm, the Fermi energy, $E_F = 0.012$ eV, still lies in the valence band. In this case, the edge response is totally overwhelmed by the bulk state in the electron transport measurements,[15,16] as it is estimated only approximately one in 10^8 electrons residing near the edge comparing with bulk.[25] Thus, it is of equal importance to investigate the transport properties of the bulk in order to interpret HgTe/CdTe QW TI overall.

In this paper, we will study the frequency dependent conductivity of the bulk of 2D topological insulator system, HgTe/CdTe QWs. In low dimensional electronic systems, electron-impurity and electron-phonon interaction can give rise to strong frequency and temperature dependence of the transport scattering time.[26,27] Here, we investigate the dynamics conductivity of HgTe/CdTe QW due to electron-random impurity interaction. Under small excitation energy, only the intra-band excitation contributes to the conductivity, since there is a significant gap lying between the conductance- and the valence-band. We will also discuss on the effect due to the temperature dependent dielectric function.

We considered an *n*-type HgTe/CdTe QW lay in the *x*-*y* plane, the thickness along *z* direction is 7.0 nm. Under a weak time-dependent electric field, $\boldsymbol{E} = \boldsymbol{E}_0 e^{-i\omega t}$, the many

a)czhang@uow.edu.au

 © 2014 AIP Publishing LLC

This article is copyrighted as indicated in the article. Reuse of AIP content is subject to the terms at: http://scitation.aip.org/termsconditions. Downloaded to IP: 130.130.37.85 On: Wed, 26 Nov 2014 03:48:51

body Hamiltonian of the system, in second quantized notation, is written as

$$H = H_0 + H^{e-e} + H^{e-I}, \tag{1}$$

$$H_0 = \sum_{\mathbf{k},s} \varepsilon_{(\mathbf{k}+\mathbf{A}),s} a^{\dagger}_{\mathbf{k},s} a_{\mathbf{k},s},$$

$$H^{e-e} = \frac{1}{2} \sum_{\mathbf{k},\mathbf{k}',q,ss's''s'''} V(q) \left[\varphi^{\dagger}_{\mathbf{k}+\mathbf{q},s} \varphi_{\mathbf{k},s'''} \varphi^{\dagger}_{\mathbf{k}'-\mathbf{q},s'} \varphi_{\mathbf{k}',s''} \right] \times a^{\dagger}_{\mathbf{k}+\mathbf{q},s} a^{\dagger}_{\mathbf{k}'-\mathbf{q},s'} a_{\mathbf{k}',s''} a_{\mathbf{k},s'''},$$

$$H^{e-I} = -Z \int d\mathbf{q} V(q) \sum_i e^{-i\mathbf{q}\cdot\mathbf{R}_i} \sum_{\mathbf{k},s} a^{\dagger}_{\mathbf{k}+\mathbf{q},s} a_{\mathbf{k},s} (\varphi^{\dagger}_{\mathbf{k}+\mathbf{q},s} \varphi_{\mathbf{k},s}).$$

Here, $\boldsymbol{A}$ in the subscription is the vector potential of the external electric field, $\boldsymbol{A} = \boldsymbol{E}_0 e^{-i\omega t}/(i\omega)$. H_0 is the non-interacting Hamiltonian of 2D system with the energy dispersion given by Ref. 28: $\varepsilon(\boldsymbol{k}) = C - Dk^2 + s\sqrt{(M - Bk^2)^2 + A^2k^2}$, where $s = \pm 1$ and A is just a parameter, which should not be confused with the vector potential written in bold style. The values of A, B, D, and M are taken from Ref. 28, for the sample 7.0 nm in thickness, which are 364.5 meV nm, -686 meV nm^2, -512 meV nm^2, and -10 meV, respectively. $H^{\text{e-e}}$ is the electron-electron interaction and $H^{\text{e-I}}$ the electron-random impurities interaction. $a^{\dagger}_{k,s}$ and $a_{k,s}$ are the creation and annihilation operators for an electron with momentum k and spin s. $V(q) = e^2/\kappa_s q$ is the Fourier transformed electron-electron Coulomb potential, κ_s is the background static dielectric constant. For CdTe, $\kappa_s = 9.4$.[29] R_i is the position of the ith ion. $\varphi_{\mathbf{k},s}$ is the wave function of an electron in the HgTe/CdTe QW.

The total average current density of the system is defined by $\boldsymbol{j} = c(\partial H/\partial \boldsymbol{A})$. To the lowest order of the electric field (linear response), the current density is given as

$$\mathbf{j}_{\mathbf{k},\alpha} = e \sum_{\mathbf{k},\alpha} (-2De\mathbf{A} - 2D\mathbf{k} + R_{\mathbf{k},s}\mathbf{k}) \langle a^{\dagger}_{\mathbf{k},\alpha} a_{\mathbf{k},\alpha} \rangle, \tag{2}$$

where,

$$R_{\mathbf{k},s} = \frac{A^2 - 2BM + 2B^2\mathbf{k}^2}{s\sqrt{(M - B\mathbf{k}^2)^2 + A^2\mathbf{k}^2}}.$$

We rewrite the total average current density in two parts (scattering-free and scattering), $\boldsymbol{j}(\omega) = \boldsymbol{j}^{sf}(\omega) + \boldsymbol{j}^{sc}(\omega)$. The scattering-free part is given as

$$\mathbf{j}^{sf}(\omega) = (-2D)\frac{ie^2}{\omega}\mathbf{E} \sum_{\mathbf{k},\alpha} \langle a^{\dagger}_{\mathbf{k},\alpha} a_{\mathbf{k},\alpha} \rangle = \left(-\frac{2mD}{\hbar^2} \right) \frac{ine^2}{m\omega}\mathbf{E} = \left(-\frac{2mD}{\hbar^2} \right) \sigma_0 \mathbf{E}, \tag{3}$$

where $\sigma_0 = ine^2/m\omega$ is the Drude conductivity in the absence of electron-impurity scattering and D is just a parameter of the material which is independent of the frequency. While $\boldsymbol{j}^{sc}(\omega)$ is the current including scattering

$$\mathbf{j}^{sc}(\omega) = e \sum_{\mathbf{k},\alpha} (-2D + R_{\mathbf{k},s})\mathbf{k} \langle a^{\dagger}_{\mathbf{k},\alpha} a_{\mathbf{k},\alpha} \rangle. \tag{4}$$

Now, let us defined the single-electron density matrix element between states $\langle \mathbf{k}, \alpha|$ and $|\mathbf{k}+\mathbf{p}, \alpha'\rangle$. Thus, $F_{\alpha'\alpha}(\mathbf{k}+\mathbf{q}, \mathbf{k}, t) = \langle a^{\dagger}_{\mathbf{k},\alpha} a_{\mathbf{k}+\mathbf{q},\alpha'} \rangle$, $\alpha = \pm 1$ corresponds to the valence and conductance band. The equation of motion for the single-electron density matrix element is[28–30]

$$\begin{aligned} i\frac{\partial}{\partial t} F_{\alpha'\alpha}(\mathbf{k}+\mathbf{p}, \mathbf{k}, t) &= \frac{1}{\hbar}[F_{\alpha'\alpha}(\mathbf{k}+\mathbf{p}, \mathbf{k}, t), H] \\ &= \frac{1}{\hbar}[\varepsilon_{(\mathbf{k}+\mathbf{p}+\mathbf{A})} - \varepsilon_{(\mathbf{k}+\mathbf{A})}] F_{\alpha'\alpha}(\mathbf{k}+\mathbf{q}, \mathbf{k}, t) \\ &\quad + \frac{1}{\hbar} \sum_{\mathbf{q}} V(\mathbf{q}) \left[n(\mathbf{q}) - Z \sum_i e^{-i\mathbf{q}\mathbf{R}_i} \right] \\ &\quad \times \left[\sum_{s=\pm 1} (\varphi^{\dagger}_{\mathbf{k}+\mathbf{q},s} \varphi_{\mathbf{k},\alpha}) F_{\alpha' s}(\mathbf{k}+\mathbf{p}, \mathbf{k}+\mathbf{q}) \right. \\ &\quad \left. - (\varphi^{\dagger}_{\mathbf{k}+\mathbf{q}',\alpha'} \varphi_{\mathbf{k}+\mathbf{p}-\mathbf{q},s}) F_{s\alpha}(\mathbf{k}+\mathbf{p}-\mathbf{q}, \mathbf{k}) \right]. \end{aligned} \tag{5}$$

We have neglected the nonlinear terms in the external field. The electron density of the system is written as

$$n(\mathbf{q}) = \sum_{s,s'=\pm 1} \left[\sum_{\mathbf{k}} \varphi^{\dagger}_{\mathbf{k},s} \varphi_{\mathbf{k}+\mathbf{q},s'} F_{s's}(\mathbf{k}+\mathbf{q}, \mathbf{k}) \right]. \tag{6}$$

Let $\mathbf{p} = 0$, the expression for $\boldsymbol{j}^{sc}(\omega)$ is given as

$$\begin{aligned} \mathbf{j}^{sc}(\omega) &= \frac{Ze}{\omega} \sum_q V(\mathbf{q}) \sum_i e^{-i\mathbf{q}\mathbf{R}_i} \\ &\quad \times \sum_{\mathbf{k},\alpha\alpha'} \left[\mathbf{k}(R_{\mathbf{k}+\mathbf{q},\alpha'} - R_{\mathbf{k},\alpha}) + \mathbf{q}(R_{\mathbf{k}+\mathbf{q},\alpha'} - 2D) \right] \\ &\quad \times \left[\left(\varphi^{\dagger}_{\mathbf{k},\alpha} \varphi_{\mathbf{k}+\mathbf{q},\alpha'} \right) F_{\alpha'\alpha}(\mathbf{k}+\mathbf{q}, \mathbf{k}) \right]. \end{aligned} \tag{7}$$

In arriving at Eq. (7), we have used the following property for an isotropic system:

$$\sum_{\mathbf{q}} \left\{ V(\mathbf{q}) n(-\mathbf{q}) \sum_{\mathbf{k}} \sum_{\alpha\alpha'} [T_{\mathbf{k}+\mathbf{q},\alpha'}(\mathbf{k}+\mathbf{q}) - T_{\mathbf{k},\alpha}\mathbf{k}] \times (\varphi^{\dagger}_{\mathbf{k},\alpha} \varphi_{\mathbf{k}+\mathbf{q},\alpha'}) F_{\alpha'\alpha}(\mathbf{k}+\mathbf{q}, \mathbf{k}) \right\} = 0.$$

We now present the main results. In the absence of the impurities and the applied field, electrons are free and are described by the Fermi-Dirac distribution, $f = \frac{1}{1+e^{\beta(\varepsilon_{\mathbf{k}}-\mu)}}$, where $\beta = 1/k_B T$, k_B is the Boltzmann constant, and μ is the chemical potential. The zeroth-order density matrix element is given as $F^{(0)}_{\alpha'\alpha}(\mathbf{k}+\mathbf{q}, \mathbf{k}, t) = f_{\mathbf{k}} \delta_{\mathbf{k},0} \delta_{\alpha'\alpha}$.

In the first order approximation, we treat the external field to be zero and determine the change of the static electron density matrix due to the impurities. From Eqs. (5) and (6), we obtain the first order density matrix self-consistently

$$F^{(1)}_{\alpha'\alpha}(\mathbf{k}+\mathbf{q}, \mathbf{k}, t) = Z \frac{f_{\mathbf{k}+\mathbf{q},\alpha'} - f_{\mathbf{k},\alpha}}{\varepsilon_{\mathbf{k}+\mathbf{q},\alpha'} - \varepsilon_{\mathbf{k},\alpha}} V(\mathbf{q}) \left[\frac{1}{\kappa(q,0)} \right] \sum_i e^{-i\mathbf{q}\cdot\mathbf{R}_i}. \tag{8}$$

This article is copyrighted as indicated in the article. Reuse of AIP content is subject to the terms at: http://scitation.aip.org/termsconditions. Downloaded to IP: 130.130.37.85 On: Wed, 26 Nov 2014 03:48:51

Here, $\kappa(q,\omega)$ the dielectric function is defined as $\kappa(q,\omega) = 1 - V(\mathbf{q})\Pi(q,\omega)$, $\Pi(q,\omega)$ is the polarization function

$$\Pi(q,\omega) = \int \frac{d\mathbf{k}}{4\pi^2} \sum_{\alpha'\alpha} \frac{|\varphi^{\dagger}_{\mathbf{k}+\mathbf{q},\alpha'}\varphi_{\mathbf{k},\alpha}|^2 (f_{\mathbf{k}+\mathbf{q},\alpha'} - f_{\mathbf{k},\alpha})}{E_{\mathbf{k}+\mathbf{q},\alpha'} - E_{\mathbf{k},\alpha} - \omega - i\delta} \quad (\delta \to 0).$$

Next, we consider the time-dependent part of the single-electron density matrix element $F^{(2)}$ under the influence of the external field and of the impurities. From $F^{(2)}$, the conductivity can be determined.[26,30,31] For the conductivity, we consider our system to be isotropic and $\boldsymbol{j}$ is parallel to $\mathbf{E}$. We also assume that the external electric field is aligned to the x direction. The current is now given as

$$j^{sc}_x(\omega) = \frac{iZne^4}{8\pi\kappa_s\omega^3} I_q(\omega) E. \tag{9}$$

$$\begin{aligned} I_q(\omega) = \int dq \frac{V(\mathbf{q})}{\kappa(q,0)} \times \Bigg\{ & \frac{V(\mathbf{q})}{\kappa(q,\omega)} \Pi_2(q,\omega) \\ & \times \left[\Pi_2(q,\omega) - \Pi_2(q,0) + q\Pi_4(q,\omega) - q\Pi_4(q,0)\right] \\ & + 2q\left[\Pi_3(q,\omega) - \Pi_3(q,0)\right] + q^2\left[\Pi_5(q,\omega) - \Pi_5(q,0)\right] \\ & + \left[\Pi_1(q,\omega) - \Pi_1(q,0)\right] - 4Dq\left[\Pi_2(q,\omega) - \Pi_2(q,0)\right] \\ & + \frac{V(\mathbf{q})}{\kappa(q,\omega)} \Pi_4(q,\omega)\left[q\Pi_2(q,\omega) - q\Pi_2(q,0)\right. \\ & \left. + q^2\Pi_4(q,\omega) - q^2\Pi_4(q,0)\right] \Bigg\}. \end{aligned} \tag{10}$$

We have the short hand notation

$$\Pi_i(q,\omega) = \sum_{\mathbf{k},\alpha\alpha'} Q_i \frac{|\varphi^{\dagger}_{\mathbf{k},\alpha}\varphi_{\mathbf{k}+\mathbf{q},\alpha'}|^2 (f_{\mathbf{k}+\mathbf{q},\alpha'} - f_{\mathbf{k},\alpha})}{(E_{\mathbf{k}+\mathbf{q},\alpha'} - E_{\mathbf{k},\alpha} - \hbar\omega)},$$

where the Q_is are the functions of k: $Q_1 = (R_{\mathbf{k}+\mathbf{q},\alpha'} - R_{\mathbf{k},\alpha})^2 k^2$, $Q_2 = (R_{\mathbf{k}+\mathbf{q},\alpha'} - R_{\mathbf{k},\alpha}) k\cos\theta_{kq}$, $Q_3 = (R_{\mathbf{k}+\mathbf{q},\alpha'} - R_{\mathbf{k},\alpha}) R_{\mathbf{k}+\mathbf{q},\alpha'} k\cos\theta_{kq}$, $Q_4 = (R_{\mathbf{k}+\mathbf{q},\alpha'} - 2D)$, and $Q_5 = (R_{\mathbf{k}+\mathbf{q},\alpha'} - 2D)^2$.

The total current density up to the second order in electron-impurity scattering is written as

$$j_x(\omega) = j^{sf}_x(\omega) + j^{sc}_x(\omega) = \left(-2m^*D - \frac{Z^2}{8\pi}\frac{r_s}{\gamma^2} I_z(\gamma)\right)\sigma_0 E. \tag{11}$$

We shall use the dimensionless notation $z = \mathrm{q}/\mathrm{k_F}$, $\gamma = \omega/\mu$. $r_s = m^* e^2/(\hbar^2 k_F)$, taking $m^* = 0.015\,m$, k_F, the Fermi wave vector, can be calculated self-consistently from carrier density. Although many terms appeared in Eq. (10), the dominant contribution is from Π_4 and Π_5. The real part of the conductivity can be written as

$$\begin{aligned} & \frac{Z^2}{8\pi}\frac{r_s}{\gamma^2}\sigma_0 E \int z^2 dz \frac{V(z)}{\kappa(z,0)} \\ & \times \left\{ \mathrm{Im}\Pi_5(z,\gamma) + \frac{V(z)\Pi_4(z,\gamma)}{\kappa(z,\gamma)}\left[\Pi_4(z,\gamma) - \Pi_4(z,0)\right] \right\}. \end{aligned}$$

Compared to a free 2D electron gas where the conductivity is solely determined by the dielectric function, the conductivity in HgTe/CdTe QW has a more complicated dependence on the electronic transitions (wavefunction overlaps and transition energies). An extra term, $(R_{\mathbf{k}+\mathbf{q},\alpha} - 2D)$, appears in the dielectric function and the conductivity. This term arises from of the velocity v at the valence band below Fermi level: $v = \frac{\partial \varepsilon_{\mathbf{k}}}{\partial k} = (-2D + R_{\mathbf{k},\alpha})k$.

In Fig. 1, we present the real part of the conductivity at two different chemical potentials at 0 K. A minimum conductivity can be found soon after a dramatic drop at low frequency regime, and then increase apparently with a very broad absorption peak. This minimum point distinguishes the intra- and inter-band excitation, and the larger Fermi energy, the higher frequency the minimum conductivity lies at, e.g., near $\omega = 0.1$ eV for $\mu = 50$ meV and near $\omega = 0.01$ eV for $\mu = 12$ meV. Under a weak excitation, intra-band excitation dominates with a very fast decrease to near zero before the inter-band contribution takes over. The inter-band excitation contribution enhanced with smaller Fermi energy, as there are more empty excited states on valence band at lower doping level, which hence raise the transition probability for the conduction electrons.

In Fig. 2, we plot the real part of conductivity of $\mu = 12$ meV, as a function of frequency at temperatures 0 K, 4 K, 77 K, and 300 K. At this frequency range which is much lower than the band gap, the conductivity is due to the contribution from intra-band excitations only. We can make some interesting observations. At fixed temperature, the conductivity decreases rapidly with the frequency at low frequency. This is consistent with the inverse power law dependence of electron-impurity scattering. The temperature dependence of the conductivity is shown in Fig. 3. At low temperature and for low frequency the conductivity decreases with the increasing temperature. This is mainly due to that the thermal excitation reduces the allowed phase space for intra-band transitions (defined by $f_{\mathbf{k}+\mathbf{q},\alpha'} - f_{\mathbf{k},\alpha}$). Thus, the electron density correlation function (the Π_i functions) decreases with the increasing temperature. Also at low frequency, the dielectric function is close to its static limit and weakly frequency dependent. As a result, the conductivity decreases as temperature increases. At high temperatures, more thermally

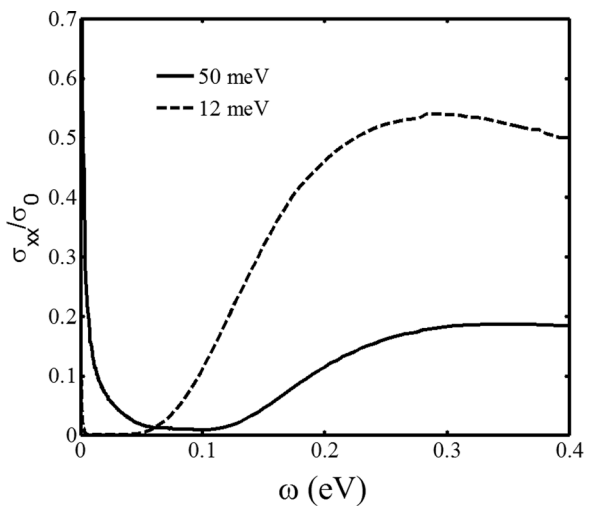

FIG. 1. The real part conductivity as a function of frequency at different chemical potential 12 meV and 50 meV, σ_0 is normalized to $n = 1 \times 10^{11}\,\mathrm{cm}^{-2}$.

This article is copyrighted as indicated in the article. Reuse of AIP content is subject to the terms at: http://scitation.aip.org/termsconditions. Downloaded to IP: 130.130.37.85 On: Wed, 26 Nov 2014 03:48:51

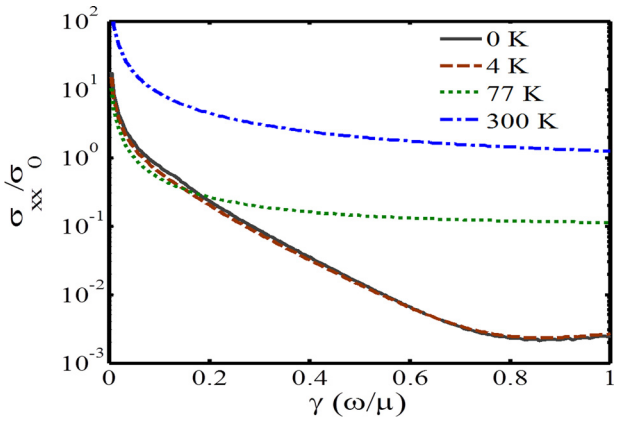

FIG. 2. The real part of the conductivity versus frequency at different temperatures with $\mu = 12$ meV.

excited carriers reduce the dynamic screen and the electron-impurity scattering is stronger. This leads to that the conductivity increases with temperature. The turnaround in the temperature dependence gives rise to a conductivity minimum in the low temperature regime. At frequency of 0.1 ω/μ, the minimum is at around 50 K, for high frequencies, the dynamical screening dominates in the whole temperature regime and conductivity increases with temperature monotonically. It is worth to point out that the temperature contribution from the dielectric function has no effect on the interband excitation, since the gap plus the Fermi energy is much larger than room temperature thermal effect.

By comparing Eq. (11) to the Drude model $\sigma = \frac{ine^2}{m^*(\omega+i/\tau)}$, the inverse scattering time can be identified, $\tau^{-1} = (Zr_s/16\pi m^* D\gamma)ImI_z(\omega)$. The frequency dependent inverse scattering time for $\mu = 12$ meV is plotted in Fig. 4. The inverse scattering time depends on the frequency very differently in the low temperature regime and in the high temperature regime. When the temperature is low, the scattering is mainly due the electrons near the Fermi surface. Electron-impurity scattering by these electrons is inversely proportional to the frequency. As frequency increases, electrons travel a shorter distance between scatterers and suffer less scattering. This picture is consistent with the Drude conductivity for degenerate electrons. In the high temperature regime, more electrons away from the Fermi level can participate in the electron-impurity scattering. These thermally excited electrons interact with

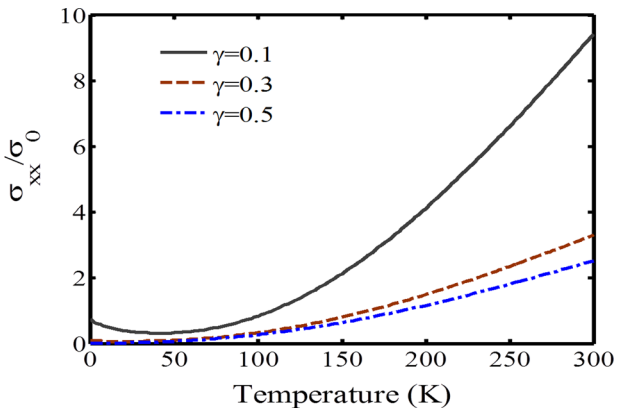

FIG. 3. The real part of the conductivity as a function of temperature for three frequencies: 1.2 meV, 3.6 meV, and 6.0 meV.

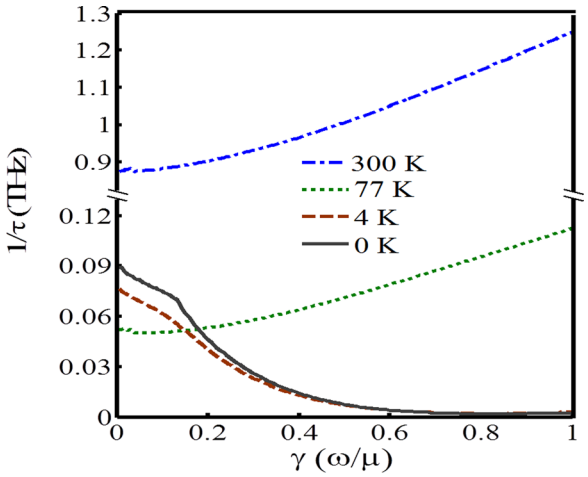

FIG. 4. Scattering rate versus frequency at four different temperatures: 0 K, 4 K, 77 K, and 300 K.

photons and impurities. As frequency increases, more thermally excited electrons from deep inside the Fermi sphere can simultaneously satisfy energy and momentum conservation required in a scattering event. As a result, the scattering rate increases with the frequency.

In summary, by using the quantum equation of motion for electron density matrix, we have calculated the frequency dependent conductivity of HgTe/CdTe QWs in the presence of random impurities. Both the frequency dependence and the temperature dependence of conductivities and the inverse scattering time are presented. The inverse transport scattering time decreases with the frequency in the low temperature regime and increases with the frequency in the high temperature regime. Our analysis is based on that the single particle scattering probability decreases with the frequency and that the number of electrons satisfying scattering condition at high temperature increase with the frequency.

The work was supported by the Australian Research Council (DP140101501), the University of Wollongong Postgraduate Scholarships, the 973 Program of China (Grant No. 2014CB339803), the 863 Program of China (Project No. 2011AA010205), and the International Collaboration and Innovation Program on High Mobility Materials Engineering of the Chinese Academy of Sciences.

[1]C. L. Kane and E. J. Mele, Phys. Rev. Lett. **95**(22), 226801 (2005).
[2]B. A. Bernevig, T. L. Hughes, and S. C. Zhang, Science **314**(5806), 1757–1761 (2006).
[3]D. Hsieh, D. Qian, L. Wray, Y. Xia, Y. S. Hor, R. J. Cava, and M. Z. Hasan, Nature **452**(7190), 970–975 (2008).
[4]Y. Xia, D. Qian, D. Hsieh, L. Wray, A. Pal, H. Lin, A. Bansil, D. Grauer, Y. S. Hor, R. J. Cava, and M. Z. Hasan, Nat. Phys. **5**(6), 398–402 (2009).
[5]D. Kim, S. Cho, N. P. Butch, P. Syers, K. Kirshenbaum, S. Adam, J. Paglione, and M. S. Fuhrer, Nat. Phys. **8**(6), 459–463 (2012).
[6]M. Konig, S. Wiedmann, C. Brune, A. Roth, H. Buhmann, L. W. Molenkamp, X. L. Qi, and S. C. Zhang, Science **318**(5851), 766–770 (2007).
[7]P. Roushan, J. Seo, C. V. Parker, Y. S. Hor, D. Hsieh, D. Qian, A. Richardella, M. Z. Hasan, R. J. Cava, and A. Yazdani, Nature **460**(7259), 1106–U1164 (2009).
[8]L. A. Wray, S. Y. Xu, Y. Q. Xia, D. Hsieh, A. V. Fedorov, Y. S. Hor, R. J. Cava, A. Bansil, H. Lin, and M. Z. Hasan, Nat. Phys. **7**(1), 32–37 (2011).
[9]M. Z. Hasan and C. L. Kane, Rev. Mod. Phys. **82**(4), 3045–3067 (2010).
[10]X. L. Qi and S. C. Zhang, Rev. Mod. Phys. **83**(4), 1057–1110 (2011).

This article is copyrighted as indicated in the article. Reuse of AIP content is subject to the terms at: http://scitation.aip.org/termsconditions. Downloaded to IP: 130.130.37.85 On: Wed, 26 Nov 2014 03:48:51

[11]N. A. Cade, J. Phys. C: Solid State Phys. **18**(26), 5135–5141 (1985).
[12]C. R. Becker, K. Ortner, X. C. Zhang, A. Pfeuffer-Jeschke, V. Latussek, Y. S. Gui, V. Daumer, H. Buhmann, G. Landwehr, and L. W. Molenkamp, Phys. E **20**(3–4), 436–443 (2004).
[13]A. A. Burkov and D. G. Hawthorn, Phys. Rev. Lett. **105**(6), 066802 (2010).
[14]A. Karch, Phys. Rev. B **83**(24), 245432 (2011).
[15]J. G. Analytis, J. H. Chu, Y. L. Chen, F. Corredor, R. D. McDonald, Z. X. Shen, and I. R. Fisher, Phys. Rev. B **81**(20), 205407 (2010).
[16]N. P. Butch, K. Kirshenbaum, P. Syers, A. B. Sushkov, G. S. Jenkins, H. D. Drew, and J. Paglione, Phys. Rev. B **81**(24), 241301 (2010).
[17]R. Schutky, C. Ertler, A. Trugler, and U. Hohenester, Phys. Rev. B **88**(19), 195311 (2013).
[18]P. Di Pietro, M. Ortolani, O. Limaj, A. Di Gaspare, V. Giliberti, F. Giorgianni, M. Brahlek, N. Bansal, N. Koirala, S. Oh, P. Calvani, and S. Lupi, Nat. Nanotechnol. **8**(8), 556–560 (2013).
[19]Q. J. Chen, Y. S. Ang, X. L. Wang, R. A. Lewis, and C. Zhang, Appl. Phys. Lett. **103**(19), 192107 (2013).
[20]D. Culcer, E. H. Hwang, T. D. Stanescu, and S. Das Sarma, Phys. Rev. B **82**(15), 155457 (2010).
[21]Y. S. Hor, A. Richardella, P. Roushan, Y. Xia, J. G. Checkelsky, A. Yazdani, M. Z. Hasan, N. P. Ong, and R. J. Cava, Phys. Rev. B **79**(19), 195208 (2009).
[22]D. Hsieh, Y. Xia, D. Qian, L. Wray, J. H. Dil, F. Meier, J. Osterwalder, L. Patthey, J. G. Checkelsky, N. P. Ong, A. V. Fedorov, H. Lin, A. Bansil, D. Grauer, Y. S. Hor, R. J. Cava, and M. Z. Hasan, Nature **460**(7259), 1101 (2009).
[23]J. G. Checkelsky, Y. S. Hor, R. J. Cava, and N. P. Ong, Phys. Rev. Lett. **106**(19), 196801 (2011).
[24]S. S. Hong, J. J. Cha, D. S. Kong, and Y. Cui, Nat. Commun. **3**, 757 (2012).
[25]N. W. Ashcroft, *Solid State Physics* (Saunders College Press, 1976).
[26]N. Tzoar and C. Zhang, Phys. Rev. B **32**(2), 1146–1151 (1985).
[27]C. Zhang and Y. Takahashi, J. Phys.: Condens. Matter **5**, 5009 (1993).
[28]M. Konig, H. Buhmann, L. W. Molenkamp, T. Hughes, C. X. Liu, X. L. Qi, and S. C. Zhang, J. Phys. Soc. Jpn. **77**(3), 031007 (2008).
[29]S. M. Sze, *Physics of Semiconductor Devices*, 2nd ed. (John Wiley and Sons, 1981).
[30]C. Zhang, Phys. Rev. B **66**(8), 081105 (2002).
[31]C. Zhang and Z. S. Ma, Phys. Rev. B **71**(12), 121307 (2005).

This article is copyrighted as indicated in the article. Reuse of AIP content is subject to the terms at: http://scitation.aip.org/termsconditions. Downloaded to IP: 130.130.37.85 On: Wed, 26 Nov 2014 03:48:51